The Astrophysical Journal Letters, 984:L56 (11pp), 2025 May 10 https://doi.org/10.3847/2041-8213/adcd6f

Star-crossed Clusters: Asteroseismic Ages for Individual Stars Are in Tension with the Ages of Their Host Clusters

Jamie Tayar[1] and Meridith Joyce[2,3]
[1] Department of Astronomy, University of Florida, Bryant Space Science Center, Stadium Road, Gainesville, FL 32611, USA
[2] Department of Physics and Astronomy, University of Wyoming, 1000 E. University Avenue, Laramie, WY 82071, USA
[3] School of Computing, University of Wyoming, 1000 E. University Avenue, Laramie, WY 82071, USA
Received 2025 February 14; revised 2025 April 11; accepted 2025 April 16; published 2025 May 6

Abstract

A meta-analysis of seismic ages determined for individual stars in the well-studied open and globular clusters NGC 6819, NGC 6791, M67, M4, M19, M80, and M9 reveals both high variance across measurements and a possible discrepancy with independent, isochrone-based age determinations for the clusters in which these stars reside. The scatter among asteroseismic ages for individual stars in any one of these clusters far surpasses both the absolute age uncertainty computed for reference cluster M92 (5.4%) and the model-to-model systematic uncertainties in isochrones (roughly 10%). This suggests that either binary processes are significantly altering the masses of stars in these clusters, or some additional corrections, perhaps as a function of mass, metallicity, or surface gravity, are required to bring the asteroseismic age scale into concordance with ages inferred from isochrone or similar model fitting.

Unified Astronomy Thesaurus concepts: Globular star clusters (656); Open star clusters (1160); Asteroseismology (73)

1. Introduction

The ages of stars are the "holy grail" of stellar demographics, enabling the study of the formation and evolution of our Galaxy. Open and globular star clusters have long served as the gold standard for stellar age determinations. Originally theorized to be groups of single stars born at the same time and formed from the same gas but spanning a range of birth masses, clusters provided ideal age calibration environments. Theoretical models of single-aged, chemically homogeneous populations, known as isochrones, are relatively straightforward to generate by interpolating over single-star stellar evolutionary tracks with different masses (e.g., A. Dotter 2016). However, a closer study of star clusters and better understanding of stellar multiplicity have revealed additional complexities. We now know that globular clusters may have significant second populations with a range of chemical compositions and possibly slightly different ages (N. Bastian & C. Lardo 2018). Open clusters may show variations in abundance within the same population though these are typically small (A. Sinha et al. 2024). Younger clusters also show spreads on the main sequence that could represent an age dispersion (e.g., A. D. Mackey & P. Broby Nielsen 2007), but these are more commonly attributed to a distribution of rotation rates, with an upper limit on the age dispersion of tens of millions of years (e.g., M. Lipatov et al. 2022). To coerce cluster data into a more idealized form suitable for model comparison, photometric (e.g., A. P. Milone et al. 2017) and spectroscopic (e.g., R. P. Schiavon et al. 2024) information can be used to separate out members with anomalous chemistry, and it is sometimes possible to identify and isolate binary stars (D. Godoy-Rivera et al. 2021a). Similarly, binary interaction products (R. D. Mathieu & A. M. Geller 2009; E. Leiner et al. 2019) can be removed to provide a more appropriate single-star sequence for estimating the cluster age using isochrones.

It is now well understood that globular and open clusters are not perfect systems with homogeneous populations, but they nonetheless remain the best objects for age determinations. By carefully collating and cleaning observational data, it is possible to use the morphology of clusters on color–magnitude diagrams to infer their ages via model fitting (e.g., D. A. Vandenberg et al. 1990; M. Salaris & A. Weiss 1998; A. Marín-Franch et al. 2009; A. Dotter et al. 2011; D. A. VandenBerg et al. 2013). By quantifying the impacts of variations in the assumptions made about the physics of stellar interiors adopted in the models, it is even possible to calculate age uncertainties from such fits (J. M. Ying et al. 2023, 2024; C. Reyes et al. 2024). Accounting likewise for uncertainties in distances, composition, nuclear reaction rates, convection physics, and so on, the best cluster ages have been shown to have absolute age uncertainties as low as 5.5% (J. M. Ying et al. 2023).

While clusters provide robust age benchmarks, the majority of stars we observe today do not reside in clusters, thus necessitating the development of a variety of other techniques to estimate stellar ages. However, most of these techniques are still fundamentally calibrated using cluster data. It is possible in some cases, for example, to use isochrones to derive ages for individual stars (noncluster members) that lie in especially sensitive regions of the Hertzsprung–Russel diagram, e.g., subgiants near or just past the main sequence turnoff (J. Tang & M. Joyce 2021; D. Godoy-Rivera et al. 2021b; M. Joyce et al. 2023). However, the reliability of isochrones in general is assessed according to their ability to fit clusters, and so the models themselves adopt clusters implicitly as ground truth (e.g., J. Choi et al. 2018).

Another age determination technique is gyrochronology, which maps the rotation periods and temperatures of stars to their ages using the fact that low-mass dwarf stars spin down over time (S. A. Barnes 2003; R. Angus et al. 2015; L. G. Bouma et al. 2024). This technique is empirically

calibrated to provide absolute rather than relative ages using rotating stars in open clusters (L. M. Rebull et al. 2018; J. L. Curtis et al. 2020). Chemical ratios may also be correlated with stellar ages, either because of the principles of galactic chemical evolution (e.g., [Y/Mg], R. da Silva et al. 2012; T. A. Berger et al. 2022) or due to internal mixing, which is traced by diagnostics such as Li (E. L. Martín et al. 2018; F. J. Galindo-Guil et al. 2022) and [C/N] (M. Martig et al. 2016; J. D. Roberts et al. 2024). Such diagnostics must be calibrated either directly on clusters (T. Spoo et al. 2022) or on intermediate results (M. H. Pinsonneault et al. 2018) that are themselves calibrated to clusters.

Another technique that has been gaining popularity for age inference on galactic scales is asteroseismology. Asteroseismology uses the global oscillation properties of a star to estimate its stellar mass (T. M. Brown et al. 1991; H. Kjeldsen & T. R. Bedding 1995). From there, it is possible to estimate an age that is significantly less sensitive to assumptions about the internal stellar physics than using, for example, luminosity and temperature (L. Morales et al. 2025). Some variations of asteroseismology try to reproduce the frequencies of individual oscillation modes to estimate extremely precise ages for targets with high-fidelity signals (V. Silva Aguirre et al. 2017; M. Joyce et al. 2024; T. Li et al. 2024; Y. Li et al. 2024), and these detailed individual mode analyses are generally expected to yield accurate and precise results (D. Huber et al. 2024; T. Li et al. 2024; J. R. Larsen et al. 2025; C. J. Lindsay et al. 2025). However, such techniques are computationally expensive and not amenable to large numbers of stars. Here we focus instead on methods that can be applied to samples of red giants large enough to perform galactic archeology. In these techniques, the observed large-frequency spacing (separation between adjacent p-modes), $\Delta\nu$, and frequency of maximum power, $\nu_{\rm max}$, are combined with information about the temperature and metallicity to estimate a stellar mass, radius, and age (e.g., J. Schonhut-Stasik et al. 2024; M. H. Pinsonneault et al. 2025). However, studies using binaries (P. Gaulme et al. 2016), open clusters (M. H. Pinsonneault et al. 2018), Gaia (Gaia Collaboration et al. 2023; J. C. Zinn et al. 2019), and models (T. R. White et al. 2011; B. Mosser et al. 2013; S. Sharma et al. 2016) have suggested that asteroseismic inferences made using simple scaling relations may not be accurate, and corrections have been developed to improve the estimated radii and masses. Work on both field populations (e.g., M. H. Pinsonneault et al. 2025) and clusters (e.g., C. Reyes et al. 2025) has emphasized the importance of careful correction and calibration in estimating accurate and precise seismic results.

It is therefore prudent to ask how current asteroseismic ages compare to cluster-based age determinations. In this analysis, we compare the ages estimated from asteroseismic analyses of individual, first-ascent red giants in well-studied open and globular clusters to the ages determined for the clusters themselves, by independent means. We describe the collation of the heterogeneous asteroseismic data from individual cluster analyses and compare the inferred ages to the cluster ages derived from isochrone fitting. We show the scale of the uncertainties from the individual scatter within clusters as well as the cluster age scale. Finally, we argue that in order to ensure that the tens to hundreds of thousands of field star ages expected from CoRoT (F. Anders et al. 2017), Kepler (M. H. Pinsonneault et al. 2025), Kepler Second Light, or K2 (A. Stokholm et al. 2023; J. T. Warfield et al. 2024), TESS (M. Hon et al. 2021; A. T. Theodoridis & J. Tayar 2023), Roman (D. Huber et al. 2023; T. J. Weiss et al. 2025), and PLATO (A. Miglio et al. 2017) are on a true and accurate scale, reanalysis of existing data and the collection of additional cluster data are required.

2. Known Uncertainties

While data do exist that could enable homogeneous cluster age determinations on a broader scale, the current literature often quotes a wide range of disparate and discrepant ages for the same cluster. Because ages are an inherently model-dependent inference, some variance in inferred cluster ages has been correctly attributed to instrumental uncertainties, modeling systematics, or the adoption of different physical assumptions within models. That said, the dispersions between quoted ages can be quite large, suggesting that additional effort to bring clusters onto a homogeneous scale may still be required. For example, for the well-studied open cluster M67, recent work cites ages from 3.8 Gyr (D. M. Nataf et al. 2024) to 4.3 Gyr (T. Cantat-Gaudin et al. 2020), and in NGC 6791, ages ranging from 6 Gyr (B. J. Anthony-Twarog & B. A. Twarog 1985) to 12 Gyr (P. B. Stetson et al. 2003) have been claimed. The metallicities quoted for a given cluster in the literature can likewise show dispersion that is often larger than the uncertainties quoted in any particular paper (see e.g., T. Wu et al. 2014a, for a more thorough indication of the diversity of ages and metallicities in the literature for any individual cluster). We can therefore say, in general, that the age inferred depends on both the model used and the method of inference (S. Byrom & J. Tayar 2024). That said, while a complete and homogeneous reanalysis of the cluster age scale across the full range of clusters (T. Cantat-Gaudin et al. 2020; E. L. Hunt & S. Reffert 2024) is a worthy goal, it represents a significant effort outside the scope of this Letter. Instead, we use in this analysis a representative age for each cluster from the recent literature, acknowledging that while scatter exists, we do not expect any individual choice to affect our result. Because we understand the true uncertainty in the cluster ages to be dominated by method-to-method scatter, we also do not propagate the individual error bars of any particular study.

Similarly, different seismic analyses of the same star will often report systematically different results for ν max and $\Delta\nu$ (M. H. Pinsonneault et al. 2018, 2025). Solar values adopted for ν max, $\Delta\nu$, and $T_{\rm eff}$ differ across analyses (M. H. Pinsonneault et al. 2018), and there are likewise different corrections (T. R. White et al. 2011; B. Mosser et al. 2013; S. Sharma et al. 2016) and different external calibrations that can be applied (J. C. Zinn et al. 2019; M. H. Pinsonneault et al. 2018, 2025). Similar to the cluster age case, the method-to-method differences in choices can have a much larger impact on the final value than the quoted random uncertainties from the individual measurements, and so we do not quote the individual uncertainties reported internally for each asteroseismic target here. In the best cases, multiple methods of analysis, including comparison between several different asteroseismic pipelines, are done on the same stars; a variety of different corrections and calibration schemes are implemented; and the uncertainties should rightfully include both the systematic differences from the methods as well as the true observational uncertainties (M. H. Pinsonneault et al. 2025). That said, while doing such an analysis for the combined cluster sample would

Table 1
Assumed Cluster Ages from Isochrone Fitting, Assumed Cluster Metallicities, the Source of the Asteroseismologyc and Whether or Not First-ascent Red Giants with Good Seismic Constraints Are Available, as Used in This Work

Cluster	Age (Gyr)	Age Source	[Fe/H]	[Fe/H] Source	Seismic Source	RGB
NGC 6819	2.54	S. Sanjayan et al. (2022)	0.03	N. Myers et al. (2022)	M. H. Pinsonneault et al. (2025)	Y
M67	3.95	C. Reyes et al. (2024)	0	N. Myers et al. (2022)	D. Stello et al. (2016)	Y
NGC 6791	8.3	K. Brogaard et al. (2012)	0.31	N. Myers et al. (2022)	M. H. Pinsonneault et al. (2025)	Y
M4	11.5	D. A. VandenBerg et al. (2013)	−1.1	M. Howell et al. (2022)	M. Howell et al. (2022)	Y
M19	12	M. Howell et al. (2025)	−1.55	M. Howell et al. (2025)	M. Howell et al. (2025)	Y
M80	13	M. Howell et al. (2024)	−1.6	M. Howell et al. (2024)	M. Howell et al. (2024)	Y
M9	13	M. Howell et al. (2025)	−1.791	M. Howell et al. (2025)	M. Howell et al. (2025)	Y
NGC 6633	0.45	R. Smiljanic et al. (2009)	−0.03	N. Lagarde et al. (2015)	N. Lagarde et al. (2015)	N
NGC 6866	0.65	T. Cantat-Gaudin et al. (2020)	0	N. Myers et al. (2022)	K. Brogaard et al. (2023)	N
Hyades	0.775	W. Brandner et al. (2023)	0.18	W. Brandner et al. (2023)	T. Arentoft et al. (2019)	N
NGC 6811	1	E. L. Sandquist et al. (2016)	−0.06	N. Myers et al. (2022)	E. L. Sandquist et al. (2016)	N
NGC 1817	1	E. L. Sandquist et al. (2020)	−0.16	N. Myers et al. (2022)	E. L. Sandquist et al. (2020)	N
NGC 2506	2.01	E. Knudstrup et al. (2020)	−0.36	E. Knudstrup et al. (2020)	E. Knudstrup et al. (2020)	N
NGC 2516	0.16	H. Sung et al. (2002)	−0.08	J. I. Bailey et al. (2018)	G. Li et al. (2024)	?

Note. The metallicities reported in this table are mainly iron abundances [Fe/H], but some are metal abundances [M/H], measurements often dominated by iron lines. We do not report α enhancements for every cluster in our table although some are α-element enhanced (see Section 3). Note that M9 is plotted at 13.2 Gyr in the figures for ease of viewing.

be extremely valuable as a future endeavor, it is a significant undertaking that is outside of the scope of this Letter.

For this Letter, we also focused specifically on first-ascent red giant stars. We expect the ages inferred for red clump and asymptotic giant branch stars, especially those at low metallicity (M. Howell et al. 2022; M. Tailo et al. 2022; M. H. Pinsonneault et al. 2025), to be extremely sensitive to our assumptions about mass loss, and so we exclude stars with those designations from our age comparison samples for all clusters.

Finally, we expect that binary interactions, either accretion or mergers that cause the star to gain mass or stripping events that cause the stars to lose mass, will also affect the inferred ages of individual stars and thus the resulting age distributions. While some such stars can be identified from asteroseismic diagnostics (e.g., S. Deheuvels et al. 2022; Y. Li et al. 2022; N. Z. Rui & J. Fuller 2024) chemical anomalies (E. Bufanda et al. 2023), rotation and activity (J. Tayar et al. 2015; T. Ceillier et al. 2017; R. A. Patton et al. 2024; D. Dixon et al. 2025), or inferred ages (M. Martig et al. 2016; C. Marasco et al. 2025), not all such stars are easily identifiable. There are also suggestions that the close binary fraction should rise at low metallicity (M. Moe et al. 2019) and that this causes a wider distribution of observed seismic masses and ages at low metallicity (J. Schonhut-Stasik et al. 2024; C. Marasco et al. 2025), which do not reflect the initial masses or true ages of these stars. Close binaries may also be more common in the cores of dense clusters for dynamical reasons (D. C. Heggie 1975; A. M. Geller & R. D. Mathieu 2012). Because of these effects, we expect that some fraction of stars in each cluster may have inferred ages that differ from the true cluster age. To address this, we use median statistics rather than means and standard deviations to report the age of each cluster; we recognize, however, that a more detailed attempt to identify individual binary interaction products in each cluster could improve future results.

3. Methods

To compare the asteroseismic age scale to the age scale from clusters, we collected data from the literature on seismic detections of first-ascent red giant branch stars in well-characterized open and globular clusters. While there are oscillation detections from other types of pulsators in clusters (T. R. Bedding et al. 2023; Y. Li et al. 2024; L. Molnár et al. 2024), we restrict our analysis to the solar-like oscillators on the first-ascent red giant branch that are the most relevant for age calibration of galactic archeology studies. This choice limits this work to the seven clusters listed in the first seven rows of Table 1. The ages and other stellar parameters for each of these stars along with their host cluster are presented in Table 2.

For M67, we assumed a cluster (i.e., isochrone-based) age of 3.95 Gyr (C. Reyes et al. 2024) and obtained seismic ages for individual red giant members from D. Stello et al. (2016) although other results do exist (e.g., T. Li et al. 2024; Y.-A. Jo & H.-Y. Chang 2024; C. Reyes et al. 2025). For NGC 6791 and NGC 6819, we used the most recent seismic ages as published in M. H. Pinsonneault et al. (2025) and membership from the OCCAM DR17 catalog (N. Myers et al. 2022), requiring a membership probability of greater than 0.3 from proper motion, radial velocity, metallicity, and T. Cantat-Gaudin et al. (2020) although again, other analyses of seismic samples do exist in the literature (e.g., S. Basu et al. 2011; S. Hekker et al. 2011; D. Stello et al. 2011a, 2011b; E. Corsaro et al. 2012; T. Wu et al. 2014b; R. Handberg et al. 2016; E. Corsaro et al. 2017; R. Handberg et al. 2017; J. M. McKeever et al. 2019; K. Brogaard et al. 2021; Ö. Çakırlı & B. Hoyman 2022; A. Covelo-Paz et al. 2023; Y.-A. Jo & H.-Y. Chang 2024). Ages for these clusters were assumed to be 8.3 Gyr (K. Brogaard et al. 2012) and 2.54 Gyr (S. Sanjayan et al. 2022), respectively. We note that while stars from NGC 6811 are also in this field and thus in the catalog, consistent with previous works (e.g., T. Arentoft et al. 2017; E. L. Sandquist et al. 2016), there were no seismic detections in first-ascent red giants that were also high-probability cluster members, and so we do not include them.

Table 2
Ages Inferred for Individual Cluster First-ascent Red Giants

ID	Mass	Logg	[M/H]	[α/M]	Teff	Cluster	Age (Gyr)
246884141	1.36	2.46	−0.1	0	5109	NGC 1817	3.69
246893162	1.29	2.35	−0.1	0	4787	NGC 1817	4.46
8000009	0.59	1.4	−1.791	0.4	4700	M80	−99
80000101	1.49	1.8	−1.791	0.4	4554	M80	1.61
80000103	0.89	1.88	−1.791	0.4	4705	M80	9.07
80000105	0.89	1.8	−1.791	0.4	4605	M80	9.08
80000107	0.85	1.45	−1.791	0.4	4454	M80	10.69
80000110	0.86	1.8	−1.791	0.4	4670	M80	10.24
80000113	0.93	1.97	−1.791	0.4	4746	M80	7.76
80000117	0.84	1.72	−1.791	0.4	4654	M80	11.14
80000120	0.79	1.91	−1.791	0.4	4739	M80	13.90
80000123	0.81	1.95	−1.791	0.4	4756	M80	12.71
80000124	0.81	1.83	−1.791	0.4	4691	M80	12.72
80000127	0.83	1.66	−1.791	0.4	4597	M80	11.64
80000128	0.76	1.69	−1.791	0.4	4666	M80	15.96
80000129	0.77	1.75	−1.791	0.4	4689	M80	15.23
80000132	0.78	1.66	−1.791	0.4	4635	M80	14.55
80000141	0.9	1.87	−1.791	0.4	4721	M80	8.73
80000190	0.77	2.1	−1.791	0.4	4834	M80	15.21
80000194	0.81	2	−1.791	0.4	4717	M80	12.71
80000199	0.75	2.13	−1.791	0.4	4846	M80	16.72
80000203	0.81	1.97	−1.791	0.4	4701	M80	12.71
80000220	0.78	1.97	−1.791	0.4	4750	M80	14.53
80000222	0.87	2.2	−1.791	0.4	4823	M80	9.80
80000234	0.87	2.02	−1.791	0.4	4811	M80	9.81
80000236	0.78	2.09	−1.791	0.4	4874	M80	14.52
8000041	0.81	1.83	−1.791	0.4	4728	M80	12.72
8000045	0.75	1.7	−1.791	0.4	4656	M80	16.75
8000046	0.77	1.73	−1.791	0.4	4643	M80	15.23
8000050	0.75	1.75	−1.791	0.4	4670	M80	16.75
8000056	0.82	1.54	−1.791	0.4	4532	M80	12.17
8000058	0.73	1.57	−1.791	0.4	4584	M80	18.51
8000068	0.76	1.49	−1.791	0.4	4567	M80	15.97
8000069	0.74	1.88	−1.791	0.4	4774	M80	17.58
4000010	0.86	2.60	−1.1	0.4	4960	M4	12.17
40000104	0.79	2.44	−1.1	0.4	4851	M4	16.81
4000011	0.71	1.93	−1.1	0.4	4612	M4	24.74
40000124	0.79	2.88	−1.1	0.4	5088	M4	16.70
40000129	0.85	2.76	−1.1	0.4	4989	M4	12.68
4000013	0.79	2.60	−1.1	0.4	4840	M4	16.83
40000130	0.85	2.48	−1.1	0.4	4897	M4	12.72
40000131	0.84	2.90	−1.1	0.4	5047	M4	13.20
40000133	0.74	1.41	−1.1	0.4	4377	M4	21.22
4000014	0.84	2.43	−1.1	0.4	4807	M4	13.29
40000142	0.89	2.78	−1.1	0.4	4988	M4	10.74
40000143	0.86	2.73	−1.1	0.4	4937	M4	12.15
40000147	0.88	2.94	−1.1	0.4	5218	M4	11.14
40000148	0.66	1.99	−1.1	0.4	4632	M4	32.55
4000015	0.68	2.16	−1.1	0.4	4865	M4	28.96
4000016	0.77	2.56	−1.1	0.4	4921	M4	18.35
40000165	0.92	2.89	−1.1	0.4	5287	M4	9.49
40000169	0.96	2.83	−1.1	0.4	5143	M4	8.13
4000017	0.92	2.62	−1.1	0.4	4785	M4	9.54
40000180	0.75	2.32	−1.1	0.4	4972	M4	20.05
40000188	0.83	2.40	−1.1	0.4	4810	M4	13.89
40000190	0.78	2.70	−1.1	0.4	4949	M4	17.54
40000191	0.77	2.52	−1.1	0.4	4892	M4	18.36
40000194	0.76	2.82	−1.1	0.4	5035	M4	19.16
40000195	0.61	1.84	−1.1	0.4	4687	M4	43.23
40000197	0.81	2.14	−1.1	0.4	4734	M4	15.24
4000020	0.85	1.94	−1.1	0.4	4535	M4	12.78
40000205	0.82	2.71	−1.1	0.4	4971	M4	14.48
4000021	0.84	2.42	−1.1	0.4	4855	M4	13.29

Table 2
(Continued)

ID	Mass	Logg	[M/H]	[α/M]	Teff	Cluster	Age (Gyr)
40000210	0.78	2.93	−1.1	0.4	5093	M4	17.44
40000213	0.82	2.64	−1.1	0.4	4836	M4	14.51
40000215	0.91	3.03	−1.1	0.4	5174	M4	9.85
40000216	0.84	2.38	−1.1	0.4	4813	M4	13.29
40000217	1.01	2.63	−1.1	0.4	5015	M4	6.80
4000022	0.75	2.46	−1.1	0.4	4852	M4	20.19
40000225	0.72	1.42	−1.1	0.4	4427	M4	23.43
40000229	0.8	2.11	−1.1	0.4	4677	M4	−99
4000023	0.76	2.54	−1.1	0.4	4897	M4	19.23
40000238	0.87	2.84	−1.1	0.4	5065	M4	11.63
4000024	0.87	2.56	−1.1	0.4	4829	M4	11.69
40000244	0.82	2.42	−1.1	0.4	4877	M4	14.52
4000025	0.78	2.20	−1.1	0.4	4719	M4	17.61
40000252	0.78	2.66	−1.1	0.4	5012	M4	17.49
4000026	0.7	1.67	−1.1	0.4	4541	M4	26.04
4000027	0.8	2.76	−1.1	0.4	4954	M4	−99
4000028	0.79	3.02	−1.1	0.4	5157	M4	16.55
4000029	0.79	2.69	−1.1	0.4	4986	M4	16.76
4000030	0.76	2.40	−1.1	0.4	4913	M4	19.19
4000031	0.81	2.67	−1.1	0.4	4966	M4	15.17
4000032	0.81	2.80	−1.1	0.4	5026	M4	15.14
4000034	0.79	2.98	−1.1	0.4	5059	M4	16.59
4000035	0.83	2.43	−1.1	0.4	4838	M4	13.89
40000358	0.77	2.34	−1.1	0.4	4814	M4	18.38
4000036	1.01	2.45	−1.1	0.4	4808	M4	6.82
40000363	0.71	1.80	−1.1	0.4	4633	M4	24.67
40000365	0.75	1.71	−1.1	0.4	4540	M4	20.20
4000037	0.85	2.46	−1.1	0.4	4821	M4	12.72
40000408	0.77	2.05	−1.1	0.4	4672	M4	18.42
4000048	0.82	2.16	−1.1	0.4	4746	M4	14.56
190000161	0.78	1.52	−1.55	0.4	4732	M19	15.12
190000162	0.84	1.55	−1.55	0.4	4610	M19	11.58
190000183	0.97	1.54	−1.55	0.4	4497	M19	6.95
190000198	0.7	1.63	−1.55	0.4	4734	M19	22.49
190000242	0.83	1.74	−1.55	0.4	4769	M19	12.09
190000247	0.8	1.84	−1.55	0.4	4897	M19	13.83
190000258	0.83	1.84	−1.55	0.4	4950	M19	12.08
190000261	0.84	1.89	−1.55	0.4	4876	M19	11.57
190000271	0.85	1.9	−1.55	0.4	4874	M19	11.08
190000276	0.72	1.81	−1.55	0.4	4891	M19	20.21
190000288	0.84	1.8	−1.55	0.4	4904	M19	11.57
190000315	0.89	1.95	−1.55	0.4	4844	M19	9.41
190000331	0.9	1.89	−1.55	0.4	4718	M19	9.06
190000335	0.85	1.93	−1.55	0.4	4829	M19	11.08
190000336	0.81	2.05	−1.55	0.4	4955	M19	13.21
190000352	0.85	2.06	−1.55	0.4	4940	M19	11.07
190000355	0.9	2.19	−1.55	0.4	4895	M19	9.04
190000357	0.85	2.43	−1.55	0.4	5112	M19	11.04
190000359	0.81	2.14	−1.55	0.4	4994	M19	13.20
190000360	0.71	2.19	−1.55	0.4	5039	M19	21.28
190000365	0.66	2.13	−1.55	0.4	4924	M19	28.04
190000366	0.67	2.33	−1.55	0.4	5095	M19	26.44
190000367	0.72	2.24	−1.55	0.4	5124	M19	20.17
190000368	0.72	2.2	−1.55	0.4	5155	M19	20.16
190000389	0.87	2.39	−1.55	0.4	5058	M19	10.16
190000392	0.89	2.13	−1.55	0.4	4918	M19	9.40
190000394	0.88	2.3	−1.55	0.4	4975	M19	9.77
190000395	0.84	2.27	−1.55	0.4	4970	M19	11.54
190000396	0.72	2.08	−1.55	0.4	4934	M19	20.22
190000399	0.8	2.24	−1.55	0.4	4949	M19	13.82
190000401	0.91	2.37	−1.55	0.4	5035	M19	8.67
190000403	0.84	2.24	−1.55	0.4	5011	M19	11.54
190000422	0.82	2.09	−1.55	0.4	5113	M19	12.61

Table 2
(Continued)

ID	Mass	Logg	[M/H]	[α/M]	Teff	Cluster	Age (Gyr)
90000103	0.71	1.4	−1.67	0.4	4618	M9	20.87
90000122	0.7	1.73	−1.67	0.4	4784	M9	22.00
90000130	0.94	1.61	−1.67	0.4	4635	M9	7.61
90000136	0.68	1.49	−1.67	0.4	4678	M9	24.53
90000137	0.91	1.77	−1.67	0.4	4601	M9	8.54
90000164	0.98	2.24	−1.67	0.4	4828	M9	6.54
90000185	0.79	2.06	−1.67	0.4	4870	M9	14.13
90000188	0.91	2.23	−1.67	0.4	4849	M9	8.50
90000189	0.83	2.44	−1.67	0.4	5110	M9	11.78
90000192	0.78	2.02	−1.67	0.4	5033	M9	14.77
90000195	0.73	2.16	−1.67	0.4	4979	M9	18.78
90000197	0.76	1.97	−1.67	0.4	4826	M9	16.23
90000198	0.73	2.26	−1.67	0.4	4865	M9	18.81
90000201	0.62	2.25	−1.67	0.4	4988	M9	34.41
90000209	0.82	2.22	−1.67	0.4	4844	M9	12.34
90000210	0.51	2.21	−1.67	0.4	5146	M9	−99
90000214	0.79	2.19	−1.67	0.4	4869	M9	14.13
90000215	0.77	2.04	−1.67	0.4	4875	M9	15.47
90000222	0.85	2.19	−1.67	0.4	4855	M9	10.83
90000223	0.93	2.28	−1.67	0.4	4818	M9	7.86
90000224	0.89	2.1	−1.67	0.4	4827	M9	9.21
9000023	0.76	1.84	−1.67	0.4	4754	M9	16.24
9000024	0.83	1.5	−1.67	0.4	4529	M9	11.84
90000240	0.76	2.3	−1.67	0.4	4994	M9	16.20
90000241	0.89	2.28	−1.67	0.4	4856	M9	9.20
90000242	0.82	2.08	−1.67	0.4	4942	M9	12.35
90000247	0.85	2.15	−1.67	0.4	4970	M9	10.83
90000248	0.87	2	−1.67	0.4	4844	M9	9.98
90000249	1.02	2.16	−1.67	0.4	4690	M9	5.70
90000250	0.69	1.97	−1.67	0.4	5107	M9	23.13
90000258	0.78	1.93	−1.67	0.4	4781	M9	14.79
90000259	1.04	2.37	−1.67	0.4	4840	M9	5.31
90000264	0.93	2.31	−1.67	0.4	4921	M9	7.86
90000281	0.87	2.06	−1.67	0.4	4799	M9	9.97
90000287	0.77	2.07	−1.67	0.4	4898	M9	15.47
90000289	0.79	1.93	−1.67	0.4	4851	M9	14.14
90000292	0.86	2.15	−1.67	0.4	4797	M9	10.39
90000295	1.13	2.3	−1.67	0.4	4976	M9	4.01
9000035	0.72	1.57	−1.67	0.4	4732	M9	19.80
9000041	0.72	1.84	−1.67	0.4	4799	M9	19.80
9000054	0.85	1.58	−1.67	0.4	4598	M9	10.86
9000066	0.74	1.94	−1.67	0.4	4900	M9	17.87
9000067	0.89	1.82	−1.67	0.4	4603	M9	9.23
9000075	0.72	1.86	−1.67	0.4	4830	M9	19.80
9000081	0.54	1.64	−1.67	0.4	4900	M9	−99
9000085	0.84	1.67	−1.67	0.4	4581	M9	11.33
9000088	0.79	1.41	−1.67	0.4	4532	M9	14.16
2436209	1.18	2.65	0.324	0.012	4424	NGC 6791	7.86
2436332	1.14	2.34	0.357	0.041	4298	NGC 6791	9.05
2569204	1.27	1.62	0.281	0.025	3926	NGC 6791	6.02
2436540	1.14	2.66	0.309	0.007	4421	NGC 6791	8.75
2569360	1.15	2.22	0.270	0.023	4260	NGC 6791	8.49
2436688	1.09	2.77	0.316	0.024	4471	NGC 6791	10.56
2436814	1.05	2.28	0.291	0.038	4299	NGC 6791	12.01
2436884	1.17	1.83	0.294	0.025	4021	NGC 6791	8.05
2436900	1.13	2.44	0.257	0.044	4363	NGC 6791	8.84
2569618	1.17	2.64	0.300	0.036	4427	NGC 6791	8.17
2437340	1.17	1.80	0.298	0.032	4020	NGC 6791	7.94
2569935	1.04	1.60	0.320	0.035	4006	NGC 6791	12.01
2437496	1.11	1.52	0.289	0.030	3898	NGC 6791	9.41
2437507	1.23	2.20	0.308	0.033	4243	NGC 6791	6.84
2437653	1.18	2.77	0.319	0.056	4534	NGC 6791	7.91
2437965	0.84	1.74	0.311	0.029	4107	NGC 6791	25.81

Table 2
(Continued)

ID	Mass	Logg	[M/H]	[α/M]	Teff	Cluster	Age (Gyr)
2570518	1.13	2.56	0.284	0.054	4456	NGC 6791	9.15
2438333	1.14	2.68	0.319	0.074	4504	NGC 6791	8.74
2708270	1.15	2.03	0.287	0.035	4165	NGC 6791	8.37
2571093	0.93	1.16	0.300	0.025	3724	NGC 6791	17.66
5111718	1.65	3.04	0.101	0.002	4901	NGC 6819	2.30
5023732	1.60	2.34	−0.004	0.012	4578	NGC 6819	2.38
5111940	1.59	2.63	0.043	0.007	4726	NGC 6819	2.50
5112072	1.65	3.01	0.039	−0.025	4886	NGC 6819	2.16
5024272	3.49	2.16	0.073	−0.008	4661	NGC 6819	0.26
5024297	1.74	2.57	0.044	0.003	4696	NGC 6819	1.90
5024583	1.78	2.48	0.034	−0.006	4652	NGC 6819	1.74
5112734	1.73	2.51	0.057	0.002	4641	NGC 6819	1.93
5112744	1.72	2.55	0.017	0.006	4676	NGC 6819	1.95
5112880	1.98	2.31	0.027	−0.008	4596	NGC 6819	1.26
5112948	1.71	2.53	0.045	0.003	4713	NGC 6819	1.98
5113061	1.53	1.54	0.031	0.005	4183	NGC 6819	2.83
4937576	1.72	2.42	0.004	0.017	4616	NGC 6819	1.90
5113441	1.69	3.10	0.078	0.019	4885	NGC 6819	2.12

Note. For each star, we have agnostically reported information as discussed in the source papers and interpolated ages in the J. Tayar et al. (2017) grid if they were not reported in the original work. ID numbers are Kepler Input Catalog IDs or TESS Input Catalog IDs where stated in the original papers. If the paper only referred to cluster members by numbers, we have appended a number related to the cluster name and several zeros before that number to avoid conflicting notation. Because of the heterogeneous nature of these sources, and the desire to understand the scatter between clusters rather than the individual uncertainties of each target, we do not report uncertainties on each column here although some may be provided in the original source.

For stars that had seismic masses but did not already have published ages, we used a grid of models optimized for the estimation of ages from first-ascent red giants published in J. Tayar et al. (2017) using the masses, surface gravities, metallicities, and α-element abundances as inputs. This method of estimating ages is in particular not sensitive to the temperature, and therefore the mixing length, assumed in the modeling (M. Joyce & J. Tayar 2023) and only sensitive at roughly the 10% level to model-to-model systematics in general (L. Morales et al. 2025). For M4, seismic ages were determined using masses, surface gravities, and temperatures presented in M. Howell et al. (2022), along with their stated metallicity of [Fe/H] $= -1.1$ and [α/Fe] $= 0.4$ for each star. We note that seismic results for some stars are also available (A. Miglio et al. 2016; M. Tailo et al. 2022; Y.-A. Jo & H.-Y. Chang 2024). The cluster age was assumed to be 11.5 Gyr (D. A. VandenBerg et al. 2013). For M80, we assumed a cluster age of 13 Gyr and masses, surface gravities, and temperatures as published in M. Howell et al. (2024), assuming their stated metallicity of [Fe/H] $= -1.791$ and [α/Fe] $= 0.4$ for each star. For M9 and M19 (M. Howell et al. 2025), we used the same procedure to turn the masses, surface gravities, assumed cluster metallicities of -1.67 and -1.55, respectively, and α-element enhancements of $+0.4$ for both clusters into ages for all of the stars listed as RGB in M. Howell et al. (2025). These were compared to cluster ages of 13 Gyr and 12 Gyr, respectively, quoted in that work. For ease of visualization on the figures, we show M9 at an age of 13.2 Gyr.

For NGC 1817, we examined two stars identified as possible red giants, adopting $\nu_{\rm max}$ and $\Delta\nu$ from E. L. Sandquist et al. (2020); one of these stars was also identified by Y.-A. Jo & H.-Y. Chang (2024). We assumed the cluster metallicity of -0.1 as stated in the E. L. Sandquist et al. (2020) paper and used the seismic scaling relations with solar values of $\nu_{\rm max,\odot} = 3090\ \mu$Hz, $\delta\nu_\odot = 135.1\ \mu$Hz, and $T_{\rm eff,\odot} = 5771.8$ K (D. Huber et al. 2011) to compute masses for these stars. However, the resulting ages were offset from the 1 Gyr age assumed for the cluster by roughly 200%. Assuming that either the evolutionary state identification for these stars is incorrect, or more careful work is needed, we exclude them from our figure.

We note that seismic measurements are also available for stars in NGC 6811 (e.g., S. Hekker et al. 2011; D. Stello et al. 2011a, 2011b; E. Corsaro et al. 2012; E. L. Sandquist et al. 2016; E. Corsaro et al. 2017; T. Arentoft et al. 2017; Y.-A. Jo & H.-Y. Chang 2024), the Hyades (M. N. Lund et al. 2016; T. Arentoft et al. 2019), NGC 6866 (K. Brogaard et al. 2023), NGC 6633 (E. Poretti et al. 2015; N. Lagarde et al. 2015), and NGC 2506 (E. Knudstrup et al. 2020). However, these clusters are young, and all of their stars are either not yet on the giant branch or have been reported being in the core helium-burning phase rather than as first-ascent red giants. This means that inferring ages requires careful treatment of advanced evolutionary stages, including and especially mass loss, that is beyond the scope of this Letter. NGC 2516 also has tentative seismic detections of three stars that may be first-ascent red giants (G. Li et al. 2024), but the published masses are outside of the grid of models we use to estimate ages, and so we do not include them in our analysis.

4. Age Comparison

In Figure 1, we compare the ages inferred from the asteroseismic analysis of each individual red giant, independent of its cluster membership, to the age inferred for the whole cluster from isochrone fitting. In the upper panel, asteroseismic age determinations for individual stars are shown as gray circles in terms of age offset, computed via [seismic age–

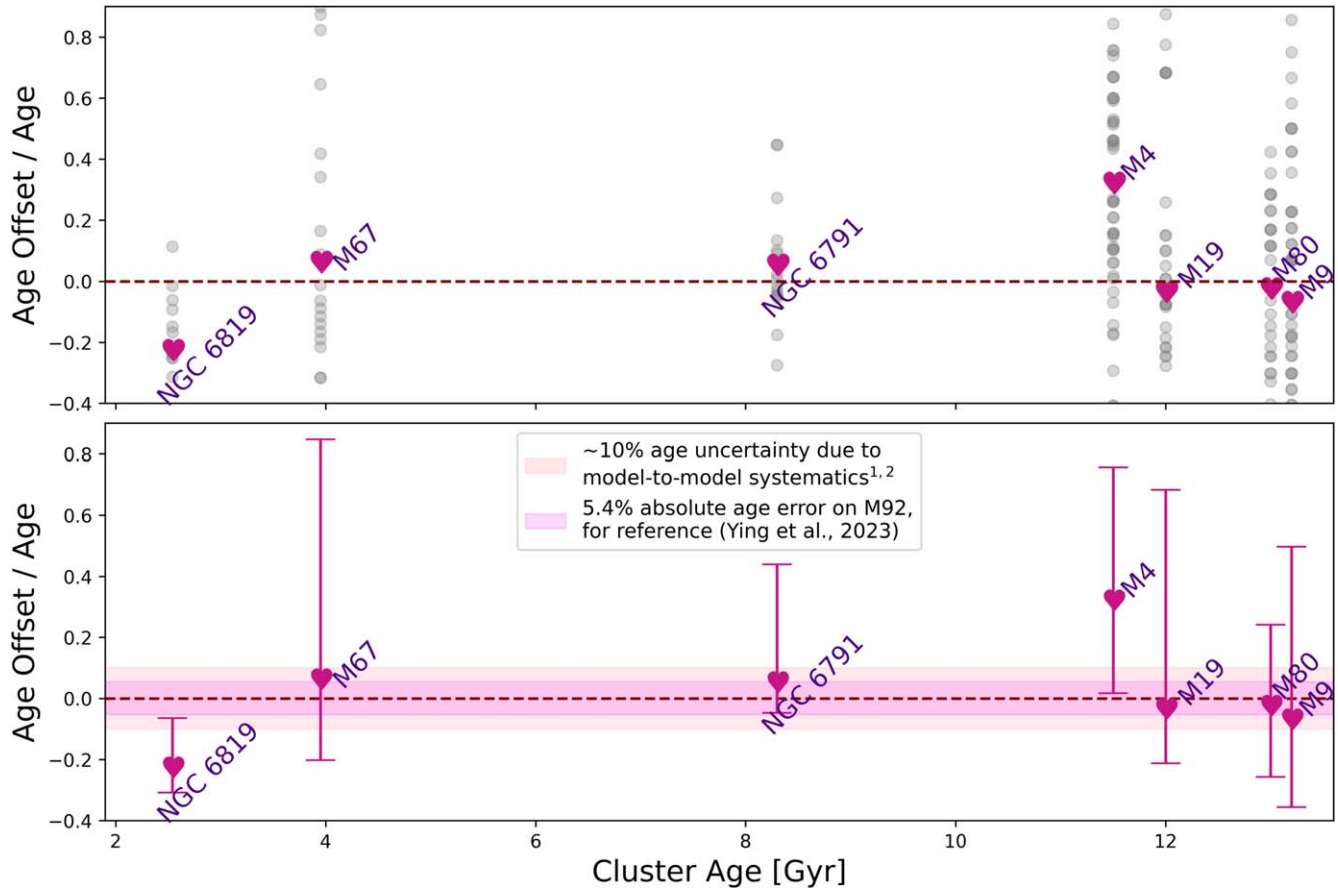

Figure 1. For seven well-characterized open and globular clusters, asteroseismic ages for individual members are compared to cluster ages derived from isochrone fitting. The colored bands represent the expected uncertainties on both the cluster age derivation (pink) and the asteroseismic age determination (orange, M. Joyce et al. 2023; M. H. Pinsonneault et al. 2025) in the optimal case. We find that the scatter for individual stars within the same cluster (gray circles) far exceeds these expected uncertainties (top). Additionally, even if we average over all the red giants in a cluster (bottom), there may be systematic offsets as a function of age, which may require future calibration. The data for M9 are artificially shifted to appear at 13.2 Gyr rather than the literature age of 13 Gyr for ease of visualization.

cluster age]/cluster age versus cluster age. In both panels, the median value among asteroseismic ages for each cluster is shown as a pink heart, as a function of cluster age. In the lower panel, asymmetric dispersions of the asteroseismic ages are shown instead of individual points. These represent the 16th and 84th quantiles and serve as a rough measure of variance among heterogeneous measurements for any particular cluster.

Notably, for some clusters, such as M67 and NGC 6791, the median age offsets are consistent within the uncertainties intrinsic to isochrone-based determinations of cluster ages (estimated to be at least 6% according to calculations for the comparable cluster M92 from J. M. Ying et al. 2023), indicated via the dark pink horizontal shaded region, or the model-to-model scatter of ages inferred this way (∼10%, M. H. Pinsonneault et al. 2025; L. Morales et al. 2025), indicated in light orange. However, for a few of the clusters, the systematic offsets between the two ages significantly exceed these uncertainties (i.e., NGC 6819, M4).

More strikingly, the dispersions among asteroseismic ages within each cluster dramatically eclipse both the model-to-model systematic uncertainties and the best-case-scenario absolute age error. These dispersions represent the spread within the cluster, which could incorporate real physical offsets from, e.g., binary processes, and therefore may not be good representations of the uncertainty on the average measurement of the cluster as a whole. That said, in all clusters but NGC 6819, asteroseismic dispersion exceeds the model-to-model systematic uncertainties by a factor of at least 5 (and a factor of 10 in the case of M67).

Although we took data from one analysis for each cluster, the inhomogeneous nature of the asteroseismic analysis and age determination methods across clusters means that it is possible that some of the offsets result from the particular method of seismic determination (M. H. Pinsonneault et al. 2018), the grid of models used (S. Byrom & J. Tayar 2024), or the heterogeneous determination of cluster ages. However, given the offsets in the median values for a few clusters, especially the well-constrained NGC 6819, we cannot rule out the existence of additional underlying systematic offsets between the cluster and asteroseismic ages scales. To determine whether such a systematic offset between the age scales is present will require isolating and removing the corrupting effects of differences in asteroseismic analysis techniques as well as a careful reinvestigation of the data within each cluster (e.g., C. Reyes et al. 2025). Systematic, homogeneous asteroseismic age determinations, ideally with the same observatory and analysis pipeline, would be a worthwhile endeavor.

5. Galactic Context

Asteroseismic ages for red giants are being used to study the properties of stars across the Milky Way and dissect the history of the Galaxy itself (V. Silva Aguirre et al. 2018; A. Stokholm

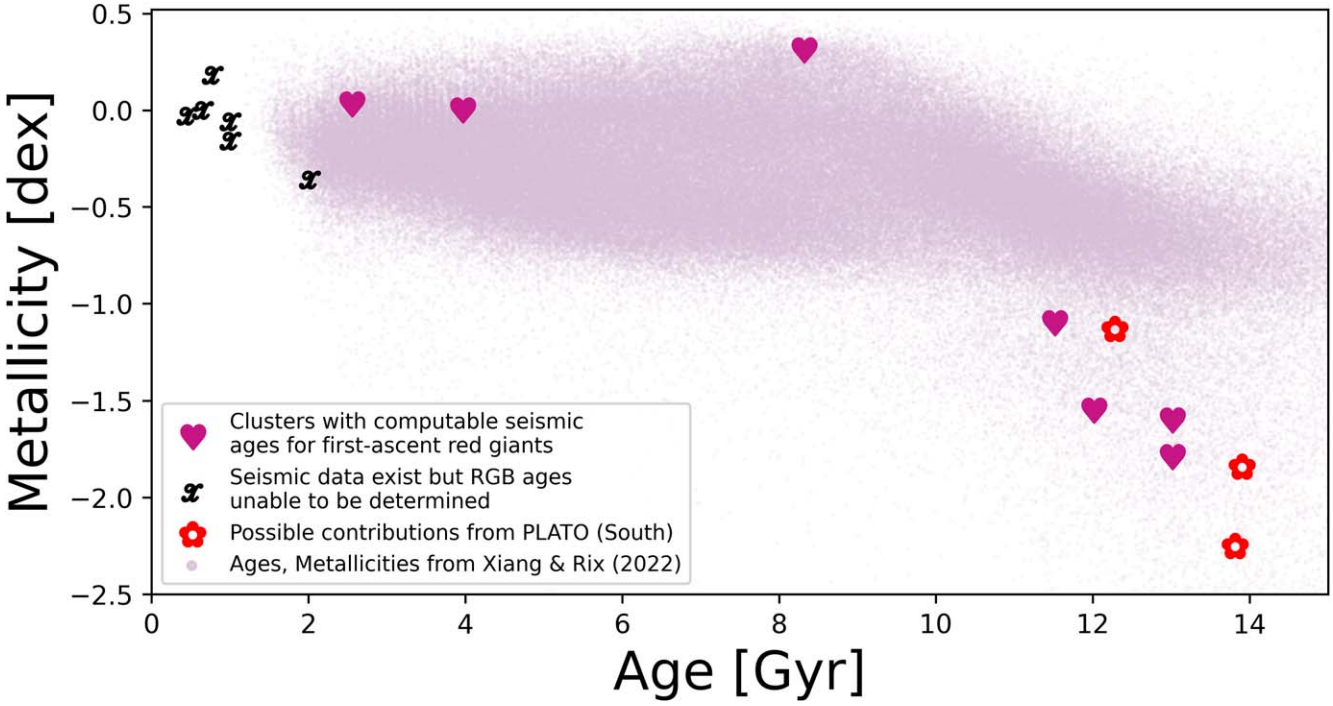

Figure 2. We show the distribution of ages for a large sample of Milky Way stars (small dots, M. Xiang & H.-W. Rix 2022) as a function of age and metallicity. The clusters that we discuss here, which can act as calibrators for the asteroseismic age estimates, are shown as pink hearts. Clusters for which any seismic data exist, even if the data is of clump stars rather than first-ascent giants, or for which we were not able to determine reliable ages, are shown as black symbols. We also mark the location of potential clusters in the upcoming PLATO mission (red flowers; see Section 5). However, we find that these cluster populations are not well distributed among the ages and metallicities of the majority of stars in the Milky Way, posing a challenge for the detailed calibration of the asteroseismic age scale.

et al. 2023), as well as serve as calibrators for other age techniques including machine learning and chemical diagnostics (e.g., M. Martig et al. 2016; M. Ness et al. 2016; H. W. Leung et al. 2023; A. Stone-Martinez et al. 2024). In particular, there is ongoing effort to understand the early formation of the Milky Way and whether significant star formation began early in the Universe (almost 14 Gyr ago) or after the peak of cosmic star formation (more like 10 Gyr ago). Unfortunately, confidently answering this question requires ages to better than 20% accuracy, and recent analyses have disagreed significantly on the age of the α-enhanced, thick disk stars in question at a significant level (V. Silva Aguirre et al. 2018; M. Xiang & H.-W. Rix 2022; A. Stokholm et al. 2023; D. M. Nataf et al. 2024). The precision of asteroseismology offers a promising way forward on this and similar questions. However, as demonstrated in Section 4, there is reason to doubt that those asteroseismic ages have been properly calibrated to the more fundamental cluster age scale at the claimed level of precision.

We also show in Figure 2 that the majority of clusters with asteroseismic data—those that could currently be used to calibrate such results—are not particularly well matched to the distribution of galactic ages and metallicities inferred from other methods (e.g., isochrone fitting of subgiants, M. Xiang & H.-W. Rix 2022). When compared to the clusters shown in this analysis (pink hearts) and all other clusters for which any seismic data exist (black markers), there are still very few constraints in the most populous parts of the age–metallicity parameter space. Figure 2 also demonstrates that future missions (e.g., PLATO, H. Rauer et al. 2014) capable of adding new clusters with asteroseismic red giant detections to this valuable sample would provide a significant advancement to the field in this context. Using the predictions from V. Nascimbeni et al. (2022), we show in Figure 2 clusters for which we anticipate receiving reliable red giant oscillation detections using ages (D. Valcin et al. 2020; J. M. Ying et al. 2023) and metallicities (R. P. Schiavon et al. 2024) from the literature. While these plans should improve the density of calibrators at old ages, there are still many regions of this parameter space devoid of calibrators.

6. Future Work

Asteroseismic ages are becoming available for large numbers of red giant stars at high precision. However, ages sit at the end of long chains of inference in stellar parameter determinations and often have systematic offsets that are challenging to constrain. Most methods for age estimation ultimately address this concern by calibrating their results to clusters, which provide the best constraints on the properties of stars of different masses. Asteroseismic data for red giants in clusters have started to become available at a range of ages and metallicities, but our initial meta-analysis of these results suggests that additional work on this topic is required. We uncovered significant dispersions among inferred ages of stars in the same cluster, as well as the possibility of systematic shifts between the average cluster age inferred from asteroseismology, and the benchmark values from isochrone fitting available in the literature. While this has been noted before in individual clusters, we show here that it is a feature broadly present across current data.

Careful analysis of a small number of high-value targets has the potential to clarify the cluster-age-scale-versus-asteroseismic-age-scale picture, separating the impacts of, e.g., binary interactions from correctable systematic offsets. Systematically derived seismic ages for just a handful of stars in well-constrained

clusters whose ages are independently determined using isochrone fitting would provide a critical calibration baseline that is currently absent from the literature, and while missions have been proposed to carry out such a study (e.g., HAYDN, A. Miglio et al. 2021), none have yet flown. In much the same way that asteroseismologists have developed corrections to the ν max scale (M. H. Pinsonneault et al. 2018) and $\Delta\nu$ scaling relation (T. R. White et al. 2011), we anticipate that asteroseismologists will determine a correction to the age scale. Development of such a correction would allow the placement of the hundreds of thousands of asteroseismic ages that are becoming available (A. Stokholm et al. 2023; J. T. Warfield et al. 2024; M. H. Pinsonneault et al. 2025; A. Theodoridis et al. 2025, in preparation) from missions like CoRoT, Kepler, K2, TESS, and soon PLATO onto an accurate scale that can be used for galactic archeology. Such studies have already begun to provide interesting insight into the relative evolution of the Milky Way disks (V. Silva Aguirre et al. 2018) and the history of Milky Way interactions (W. J. Chaplin et al. 2020; S. K. Grunblatt et al. 2021). Placing huge numbers of stars on a reliable absolute scale will enable us to constrain the evolutionary history of the Milky Way and unlock new understanding about the star formation, chemical enrichment, and merger history of our galactic home.

Acknowledgments

J.T. and M.J. contributed equally to this manuscript and may both refer to this as a first-author publication. J.T. would like to thank the UF Astraeus Space Institute for financial support for this effort. J.T. would also like to thank Open Cluster Journal Club and Russel White for helpful cluster thoughts, and Susie Byrom for her M67 literature review. J.T. and M.J. wish to thank Sarah Ballard, Alex Camazon, Zach Claytor, Isabel Colman, Jason Dittman, Anthony Gonzalez, Rafael Guzman, Corin Marasco, and Joel Zinn for helpful discussions about cluster seismology. We also thank the anonymous referee, C. Reyes, and T. Wagg for helpful suggestions that improved the manuscript.

ORCID iDs

Jamie Tayar https://orcid.org/0000-0002-4818-7885
Meridith Joyce https://orcid.org/0000-0002-8717-127X

References

Anders, F., Chiappini, C., Rodrigues, T. S., et al. 2017, A&A, 597, A30
Angus, R., Aigrain, S., Foreman-Mackey, D., & McQuillan, A. 2015, MNRAS, 450, 1787
Anthony-Twarog, B. J., & Twarog, B. A. 1985, ApJ, 291, 595
Arentoft, T., Brogaard, K., Jessen-Hansen, J., et al. 2017, ApJ, 838, 115
Arentoft, T., Grundahl, F., White, T. R., et al. 2019, A&A, 622, A190
Bailey, J. I., Mateo, M., White, R. J., Shectman, S. A., & Crane, J. D. 2018, MNRAS, 475, 1609
Barnes, S. A. 2003, ApJ, 586, 464
Bastian, N., & Lardo, C. 2018, ARA&A, 56, 83
Basu, S., Grundahl, F., Stello, D., et al. 2011, ApJL, 729, L10
Bedding, T. R., Murphy, S. J., Crawford, C., et al. 2023, ApJL, 946, L10
Berger, T. A., van Saders, J. L., Huber, D., et al. 2022, ApJ, 936, 100
Bouma, L. G., Hillenbrand, L. A., Howard, A. W., et al. 2024, ApJ, 976, 234
Brandner, W., Calissendorff, P., & Kopytova, T. 2023, AJ, 165, 108
Brogaard, K., Arentoft, T., Jessen-Hansen, J., & Miglio, A. 2021, MNRAS, 507, 496
Brogaard, K., Arentoft, T., Miglio, A., et al. 2023, A&A, 679, A23
Brogaard, K., VandenBerg, D. A., Bruntt, H., et al. 2012, A&A, 543, A106
Brown, T. M., Gilliland, R. L., Noyes, R. W., & Ramsey, L. W. 1991, ApJ, 368, 599
Bufanda, E., Tayar, J., Huber, D., Hasselquist, S., & Lane, R. R. 2023, ApJ, 959, 123
Byrom, S., & Tayar, J. 2024, RNAAS, 8, 201
Çakırlı, Ö., & Hoyman, B. 2022, MNRAS, 509, 5511
Cantat-Gaudin, T., Anders, F., Castro-Ginard, A., et al. 2020, A&A, 640, A1
Ceillier, T., Tayar, J., Mathur, S., et al. 2017, A&A, 605, A111
Chaplin, W. J., Serenelli, A. M., Miglio, A., et al. 2020, NatAs, 4, 382
Choi, J., Conroy, C., Ting, Y.-S., et al. 2018, ApJ, 863, 65
Corsaro, E., Mathur, S., García, R. A., et al. 2017, A&A, 605, A3
Corsaro, E., Stello, D., Huber, D., et al. 2012, ApJ, 757, 190
Covelo-Paz, A., Themeßl, N., Espinoza-Rojas, F., & Hekker, S. 2023, A&A, 679, A134
Curtis, J. L., Agüeros, M. A., Matt, S. P., et al. 2020, ApJ, 904, 140
da Silva, R., Porto de Mello, G. F., Milone, A. C., et al. 2012, A&A, 542, A84
Deheuvels, S., Ballot, J., Gehan, C., & Mosser, B. 2022, A&A, 659, A106
Dixon, D., Stassun, K. G., Mathieu, R. D., Tayar, J., & Cao, L. 2025, arXiv:2504.05561
Dotter, A. 2016, ApJS, 222, 8
Dotter, A., Sarajedini, A., & Anderson, J. 2011, ApJ, 738, 74
Gaia Collaboration, Vallenari, A., Brown, A. G. A., et al. 2023, A&A, 674, A1
Galindo-Guil, F. J., Barrado, D., Bouy, H., et al. 2022, A&A, 664, A70
Gaulme, P., McKeever, J., Jackiewicz, J., et al. 2016, ApJ, 832, 121
Geller, A. M., & Mathieu, R. D. 2012, AJ, 144, 54
Godoy-Rivera, D., Pinsonneault, M. H., & Rebull, L. M. 2021a, ApJS, 257, 46
Godoy-Rivera, D., Tayar, J., Pinsonneault, M. H., et al. 2021b, ApJ, 915, 19
Grunblatt, S. K., Zinn, J. C., Price-Whelan, A. M., et al. 2021, ApJ, 916, 88
Handberg, R., Brogaard, K., Miglio, A., et al. 2017, MNRAS, 472, 979
Handberg, R., Miglio, A., Brogaard, K., Bossini, D., & Elsworth, Y. P. 2016, AN, 337, 799
Heggie, D. C. 1975, MNRAS, 173, 729
Hekker, S., Basu, S., Stello, D., et al. 2011, A&A, 530, A100
Hon, M., Huber, D., Kuszlewicz, J. S., et al. 2021, ApJ, 919, 131
Howell, M., Campbell, S. W., Kalup, C., Stello, D., & De Silva, G. M. 2025, MNRAS, 536, 1389
Howell, M., Campbell, S. W., Stello, D., & De Silva, G. M. 2022, MNRAS, 515, 3184
Howell, M., Campbell, S. W., Stello, D., & De Silva, G. M. 2024, MNRAS, 527, 7974
Huber, D., Bedding, T. R., Stello, D., et al. 2011, ApJ, 743, 143
Huber, D., Pinsonneault, M., Beck, P., et al. 2023, arXiv:2307.03237
Huber, D., Slumstrup, D., Hon, M., et al. 2024, ApJ, 975, 19
Hunt, E. L., & Reffert, S. 2024, A&A, 686, A42
Jo, Y.-A., & Chang, H.-Y. 2024, NewA, 113, 102290
Joyce, M., Johnson, C. I., Marchetti, T., et al. 2023, ApJ, 946, 28
Joyce, M., Molnár, L., Cinquegrana, G., et al. 2024, ApJ, 971, 186
Joyce, M., & Tayar, J. 2023, Galax, 11, 75
Kjeldsen, H., & Bedding, T. R. 1995, A&A, 293, 87
Knudstrup, E., Grundahl, F., Brogaard, K., et al. 2020, MNRAS, 499, 1312
Lagarde, N., Miglio, A., Eggenberger, P., et al. 2015, A&A, 580, A141
Larsen, J. R., Rørsted, J. L., Aguirre Børsen-Koch, V., et al. 2025, arXiv:2503.23063
Leiner, E., Mathieu, R. D., Vanderburg, A., Gosnell, N. M., & Smith, J. C. 2019, ApJ, 881, 47
Leung, H. W., Bovy, J., Mackereth, J. T., & Miglio, A. 2023, MNRAS, 522, 4577
Li, G., Aerts, C., Bedding, T. R., et al. 2024, A&A, 686, A142
Li, T., Bi, S., Davies, G. R., et al. 2024, MNRAS, 530, 2810
Li, Y., Bedding, T. R., Huber, D., et al. 2024, ApJ, 974, 77
Li, Y., Bedding, T. R., Murphy, S. J., et al. 2022, NatAs, 6, 673
Lindsay, C. J., Ong, J. M. J., García, R. A., et al. 2025, AAS Journals, submitted
Lipatov, M., Brandt, T. D., & Gossage, S. 2022, ApJ, 934, 105
Lund, M. N., Basu, S., Silva Aguirre, V., et al. 2016, MNRAS, 463, 2600
Mackey, A. D., & Broby Nielsen, P. 2007, MNRAS, 379, 151
Marasco, C., Tayar, J., & Nidever, D. 2025, AJ, in press
Marín-Franch, A., Aparicio, A., Piotto, G., et al. 2009, ApJ, 694, 1498
Martig, M., Fouesneau, M., Rix, H.-W., et al. 2016, MNRAS, 456, 3655
Martín, E. L., Lodieu, N., Pavlenko, Y., & Béjar, V. J. S. 2018, ApJ, 856, 40
Mathieu, R. D., & Geller, A. M. 2009, Natur, 462, 1032
McKeever, J. M., Basu, S., & Corsaro, E. 2019, ApJ, 874, 180
Miglio, A., Chaplin, W. J., Brogaard, K., et al. 2016, MNRAS, 461, 760
Miglio, A., Chiappini, C., Mosser, B., et al. 2017, AN, 338, 644
Miglio, A., Girardi, L., Grundahl, F., et al. 2021, ExA, 51, 963
Milone, A. P., Piotto, G., Renzini, A., et al. 2017, MNRAS, 464, 3636
Moe, M., Kratter, K. M., & Badenes, C. 2019, ApJ, 875, 61
Molnár, L., Netzel, H., Howell, M., Kalup, C., & Joyce, M. 2024, arXiv:2409.05391
Morales, L., Tayar, J., & Claytor, Z. 2025, AJ, submitted

Mosser, B., Michel, E., Belkacem, K., et al. 2013, A&A, 550, A126
Myers, N., Donor, J., Spoo, T., et al. 2022, AJ, 164, 85
Nascimbeni, V., Piotto, G., Börner, A., et al. 2022, A&A, 658, A31
Nataf, D. M., Schlaufman, K. C., Reggiani, H., & Hahn, I. 2024, ApJ, 976, 87
Ness, M., Hogg, D. W., Rix, H. W., et al. 2016, ApJ, 823, 114
Patton, R. A., Pinsonneault, M. H., Cao, L., et al. 2024, MNRAS, 528, 3232
Pinsonneault, M. H., Elsworth, Y. P., Tayar, J., et al. 2018, ApJS, 239, 32
Pinsonneault, M. H., Zinn, J. C., Tayar, J., et al. 2025, ApJS, 276, 69
Poretti, E., Mathias, P., Barban, C., et al. 2015, in Astrophysics and Space Science Proc. 39, Asteroseismology of Stellar Populations in the Milky Way (Berlin: Springer), 101
Rauer, H., Catala, C., Aerts, C., et al. 2014, ExA, 38, 249
Rebull, L. M., Stauffer, J. R., Cody, A. M., et al. 2018, AJ, 155, 196
Reyes, C., Stello, D., Hon, M., et al. 2024, MNRAS, 532, 2860
Reyes, C., Stello, D., Hon, M., et al. 2025, MNRAS, 538, 1720
Roberts, J. D., Pinsonneault, M. H., Johnson, J. A., et al. 2024, MNRAS, 530, 149
Rui, N. Z., & Fuller, J. 2024, OJAp, 7, 81
Salaris, M., & Weiss, A. 1998, A&A, 335, 943
Sandquist, E. L., Jessen-Hansen, J., Shetrone, M. D., et al. 2016, ApJ, 831, 11
Sandquist, E. L., Stello, D., Arentoft, T., et al. 2020, AJ, 159, 96
Sanjayan, S., Baran, A. S., Németh, P., & Kinemuchi, K. 2022, AcA, 72, 267
Schiavon, R. P., Phillips, S. G., Myers, N., et al. 2024, MNRAS, 528, 1393
Schonhut-Stasik, J., Zinn, J. C., Stassun, K. G., et al. 2024, AJ, 167, 50
Sharma, S., Stello, D., Bland-Hawthorn, J., Huber, D., & Bedding, T. R. 2016, ApJ, 822, 15
Silva Aguirre, V., Bojsen-Hansen, M., Slumstrup, D., et al. 2018, MNRAS, 475, 5487
Silva Aguirre, V., Lund, M. N., Antia, H. M., et al. 2017, ApJ, 835, 173
Sinha, A., Zasowski, G., Frinchaboy, P., et al. 2024, ApJ, 975, 89
Smiljanic, R., Gauderon, R., North, P., et al. 2009, A&A, 502, 267
Spoo, T., Tayar, J., Frinchaboy, P. M., et al. 2022, AJ, 163, 229
Stello, D., Huber, D., Kallinger, T., et al. 2011a, ApJL, 737, L10
Stello, D., Meibom, S., Gilliland, R. L., et al. 2011b, ApJ, 739, 13
Stello, D., Vanderburg, A., Casagrande, L., et al. 2016, ApJ, 832, 133
Stetson, P. B., Bruntt, H., & Grundahl, F. 2003, PASP, 115, 413
Stokholm, A., Aguirre Børsen-Koch, V., Stello, D., Hon, M., & Reyes, C. 2023, MNRAS, 524, 1634
Stone-Martinez, A., Holtzman, J. A., Imig, J., et al. 2024, AJ, 167, 73
Sung, H., Bessell, M. S., Lee, B.-W., & Lee, S.-G. 2002, AJ, 123, 290
Tailo, M., Corsaro, E., Miglio, A., et al. 2022, A&A, 662, L7
Tang, J., & Joyce, M. 2021, RNAAS, 5, 117
Tayar, J., Ceillier, T., García-Hernández, D. A., et al. 2015, ApJ, 807, 82
Tayar, J., Somers, G., Pinsonneault, M. H., et al. 2017, ApJ, 840, 17
Theodoridis, A. T., & Tayar, J. 2023, RNAAS, 7, 148
Valcin, D., Bernal, J. L., Jimenez, R., Verde, L., & Wandelt, B. D. 2020, JCAP, 2020, 002
Vandenberg, D. A., Bolte, M., & Stetson, P. B. 1990, AJ, 100, 445
VandenBerg, D. A., Brogaard, K., Leaman, R., & Casagrande, L. 2013, ApJ, 775, 134
Warfield, J. T., Zinn, J. C., Schonhut-Stasik, J., et al. 2024, AJ, 167, 208
Weiss, T. J., Downing, N. J., Pinsonneault, M. H., et al. 2025, arXiv:2503.04999
White, T. R., Bedding, T. R., Stello, D., et al. 2011, ApJ, 743, 161
Wu, T., Li, Y., & Hekker, S. 2014a, ApJ, 786, 10
Wu, T., Li, Y., & Hekker, S. 2014b, ApJ, 781, 44
Xiang, M., & Rix, H.-W. 2022, Natur, 603, 599
Ying, J. M., Chaboyer, B., Boudreaux, E. M., et al. 2023, AJ, 166, 18
Ying, J. M., Chaboyer, B., & Du, W. 2024, ApJ, 970, 184
Zinn, J. C., Pinsonneault, M. H., Huber, D., et al. 2019, ApJ, 885, 166